Journal of The Electrochemical Society, **156** (12) K223-K226 (2009)
0013-4651/2009/156(12)/K223/4/$25.00 © The Electrochemical Society

Electrical Properties of Mesoporous Silicon: From a Surface Effect to Coulomb Blockade and More

L. Boarino,[*,z] S. Borini, and G. Amato

Electromagnetic Division, Istituto Nazionale Ricerca Metrologica, Turin 10135, Italy

Since the publication of the paper of [V. Lehmann, F. Hofmann, F. Moeller, and U. Gruening, *Thin Solid Films*, **255**, 20 (1995)], a great deal of effort has been produced to understand the basic mechanisms ruling the electron transport in Si mesostructures and how these phenomena are affected by the external environment. After more than 10 years of studies on mesoporous silicon in interaction with gas molecules, the latest experimental evidences and physical insights have been revealed, such as gas sensitivity, chemisorption phenomena, coulomb blockade, and glassy dynamics at room temperature. But by reading that former paper, the feeling of an extraordinary comprehension and intuition of the physical mechanisms occurring in this fascinating material continuously accompanied the reader. A review of these major results, starting from the first evidence of a strong interaction with nitrogen dioxide, to the in situ Fourier transform IR and electron paramagnetic resonance spectroscopy studies, and to the more recent electronic transport experiments on this material was reported, which follows Lehmann's intuitions in his paper.
 [DOI: 10.1149/1.3232202]

Manuscript submitted January 13, 2009; revised manuscript received August 11, 2009. Published October 7, 2009. This was Paper 1825 presented at the Honolulu, Hawaii, Meeting of the Society, October 12–17, 2008.

In the first half of the 1990s, the most studied porous silicon morphology was from high resistivity p-type wafers due to their high luminescence efficiency. The former studies on the electrical and transport properties of nano-[1] and mesoporous[2] silicon (mesoPS) revealed that the resistivity of the porous layer was a few orders of magnitude higher than in the original substrate. The models proposed at that time to explain these results were based on quantum confinement[3] and on the dielectric constant variation,[4] but they were strictly applicable to luminescent confined structures, rather than to mesoPS from a highly doped silicon. Lehmann's paper on the electrical properties of porous silicon in p+ doped wafers[5] addressed some unanswered crucial questions regarding resistivity, impurity role, carrier freeze-out, and surface conditioning. Because the structure of mesoPS has a broad size distribution ranging between 4 and 12 nm,[6] a strong room-temperature luminescence caused by quantum confinement is not observed. In his paper, Lehmann proposed a microscopic model of transport in mesoPS in which trapped charges at the surface could result in the blocking of the conduction mechanisms. Starting from this former work, a study of almost 10 years on IR spectroscopy, electron spin resonance, and electrical transport in interaction with two probe gases, nitrogen dioxide and ammonia, leads to the direct observation and comprehension of the basic mechanisms ruling the electrical transport in mesoPS, such as free carrier reactivation, chemisorption, coulomb blockade, and more. This paper is a review of these main results.

High Resistivity of MesoPS

One of the most inspiring ideas in Lehmann's paper is the analogy of mesoPS structures to submicrometer channels of complementary metal oxide semiconductor (CMOS) devices, whose figures of telegraph noise are due to the single charge trapping at the oxide–semiconductor interface. Telegraph noise is a screening effect manifesting in submicrometer CMOS channels,[7] ascribable to the capture and emission from a trap at the silicon–oxide interface in the gate region, blocking a part of the channel to electrical conduction. A parallel of silicon nanowires in a mesoporous structure was proposed, in which charged surface traps could block the conduction pathways by coulomb repulsion.

Another evidence in support of this hypothesis was the almost complete transparence to IR light of the material after etching, while in the original form the highly doped substrates were opaque due to the absorption of free carriers. So, the question was like how Polisski et al.[8] titled one of their papers: "Boron in Mesoporous Si: Where Have all the Carriers Gone?"

In this work, the authors proposed, on the basis of a detailed elastic recoil detection analysis and secondary-ion mass spectrometry studies, that despite the electrical and optical evidence of the complete absence of free carriers, boron is still present after etching and that the electrochemical process does not selectively remove these impurities (vice versa at high porosities; the boron content increases with respect to silicon atoms) so the most plausible explanation resides in the presence of saturated dangling bonds. These centers, also called P_b centers,[9] have been observed through electron spin resonance (ESR) by different groups[10,11] and could be the reason for the high resistivity of mesoPS. These authors also proposed a mechanism affecting the mesoPS formation and morphology, in which B impurities remain passivated in near-surface sites, while the etching proceeds in removing silicon atoms that are not in the vicinity of the impurities. This picture could also justify the different size distribution of crystallites in mesoPS.

Surface Effects

To validate his model, Lehmann also focused his attention on the interaction between a mesoPS and the environment in polar gases and liquids such as water and ethanol.[7] The condensation of these two vapors or the direct immersion in these two liquids gave origin to an increase in conductivity, explained by Tsu and Babic[4] through an increase in the effective dielectric constant. The interaction with liquid methanol was then addressed by a detailed study of Timoshenko et al.[12]

In the same period, the first report of the sensitivity of porous silicon (PS) to NO_2 appeared in literature by Harper and Sailor.[13] They used an n-type nanoporous silicon obtained by front illumination, but the effect of exposure to nitrogen dioxide was not reversible.

MesoPS and Nitrogen Dioxide

In 1999, our group[14] announced the observation of a strong interaction between a mesoporous p+ silicon and nitrogen dioxide at European Material Research Society Meeting, Strasbourg, where Volker Lehmann was the chairman, and he was sincerely interested in the electrical and IR striking response of this material to nitrogen dioxide.

In Fig. 1 (left), the current response of different porosity samples of mesoPS, contacted by chromium gold pads in planar configuration, is shown and plotted vs exposure time. The right axis reports

* Electrochemical Society Active Member.
[z] E-mail: l.boarino@inrim.it

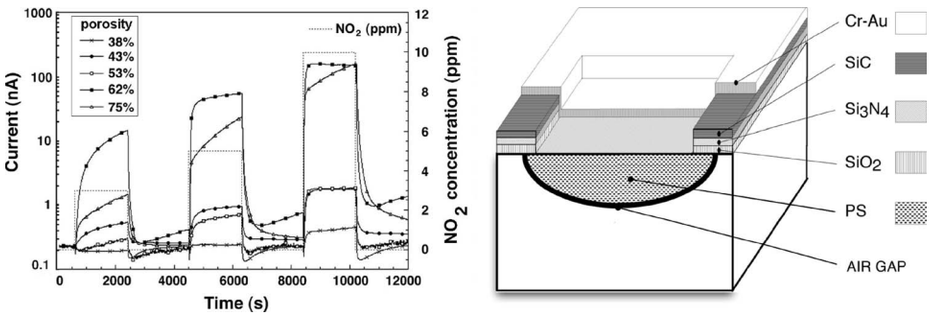

Figure 1. (Left) Electrical response to the controlled concentrations of NO_2 (3, 5, and 10 ppm) of one of the former group of mesoPS sensors as a function of time and plotted for increasing porosities. (Right) The fabrication scheme of a front-side micromachined mesoPS sensor.

the NO_2 concentration, and the thin continuous line refers to the different gas dosage in the chamber. The samples were constantly biased at 5 V.

The response is apparently related to the specific surface through porosity, with a maximum of around 62%, as reported by previous studies,[15] but we assumed that the structure's dimensions are more meaningful than its porosity. The response to gas was impressive, more than 1 order of magnitude in the current variation of 1 ppm, a sensitivity that has never been reported with any other gas or liquids. Another striking feature of the data was the response time, which was composed of a sharp and quick response on the rising front, and a slower component that never reaches stability or saturation in the flat part of the step. During gas evacuation, a peculiar and undesired drift in the response was also observed on the visualized time scale.

While a technological CMOS-compatible process was easily proposed in 2001[16] for the front-side fabrication of a porous silicon NO_2 sensor, the origin of a different record of high sensitivity obtained by a self-suspended membrane of PS (Fig. 1, right) was still unclear. The active element, mesoPS, was obtained by opening a window in the passivation layers, then performing an electrochemical etching of the mesoPS formation, and stopping the etching with a few seconds of high current density, working in an electropolishing regime. The mesoporous membrane obtained is then suspended by using the passivation layer.

In Fig. 2, the electrical response of a front-side micromachined NO_2 sensor is presented. The comparison between the electrical response of a suspended-membrane PS sensor and a PS layer in contact with the crystalline substrate is shown for different NO_2 concentrations from 200 ppb (alarm level for EU legislation)[17,18] to 10 ppm. More than 2 orders of magnitude in relative conductance $(G - G_0)/G_0$ in the presence of 1 ppm of NO_2 was obtained with respect to the normal configuration. These first indications on the response of freestanding and electrically insulated structures were important to improve the device performances, but the origin of the reactivity was still unclear.

FTIR Studies

In conjunction with the investigation on the electrical properties, in situ IR spectroscopy was carried out, revealing another impressive feature of the interaction phenomenon. The Fourier transform infrared (FTIR) spectra of freshly prepared mesoPS have been widely reported in Ref. 19, but a study of the spectral evolution in a controlled environment was still lacking. The first FTIR measurements of fresh mesoPS in the presence of NO_2 were impressive because a featureless absorption, characteristic of a loss of transparency in the sample, occurred at the NO_2 exposure with an almost fully reversible effect during the gas evacuation. The typical spectral features related to the Si–H_x stretching and SiO–H modes were apparently not affected by this dramatic optical response. This behavior is shown in Fig. 3, where the solid line 1 is the spectrum of the fresh sample in the vacuum, the dashed line 2 is the spectrum in the presence of 1 Torr of pure NO_2, and the dotted line 3 is the spectrum acquired after gas evacuation. The complete recovery of the initial conditions (curve 1) only after air exposure is not yet fully understood.

This loss of transparency was immediately attributed to the optical absorption of the free carriers, reactivated in some way by its interaction with NO_2, a molecule with a rather high electron affinity (2.2 eV).

Then, the following years were devoted to a fundamental study of mesoPS in interaction with gas by IR spectroscopy,[20,21] ESR,[22] NMR, and ab initio calculations[23,24] to understand the basic mechanisms at the origin of such an impressive optical and electrical response to nitrogen dioxide. Other gases have been employed as

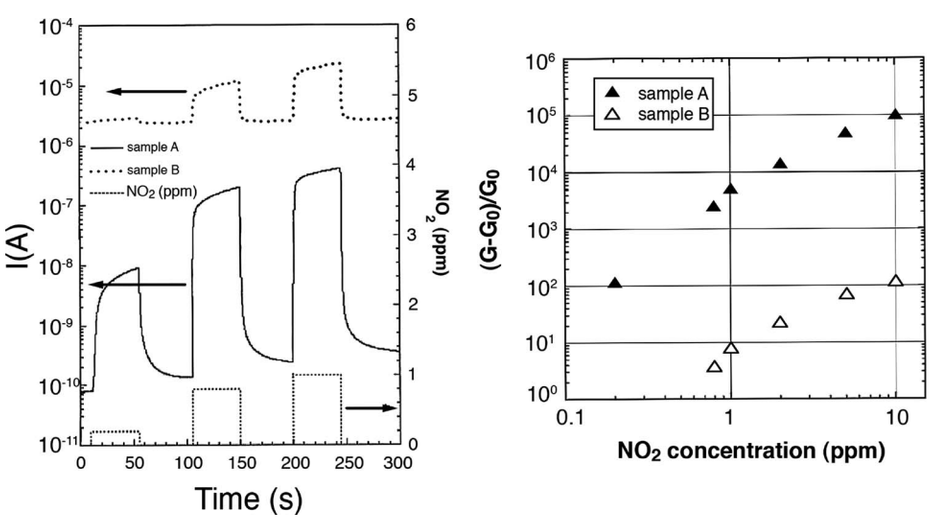

Figure 2. (Left) Electrical response vs time of a front-side micromachined NO_2 sensor with a NO_2 dosage of 200 ppb, 800 ppb, and 1 ppm. (Right) A comparison between the electrical response of a suspended-membrane PS sensor (sample A) and a PS layer still attached to the crystalline substrate is shown (sample B) for NO_2 concentrations ranging from 200 ppb (alarm level for EU legislation) to 10 ppm.

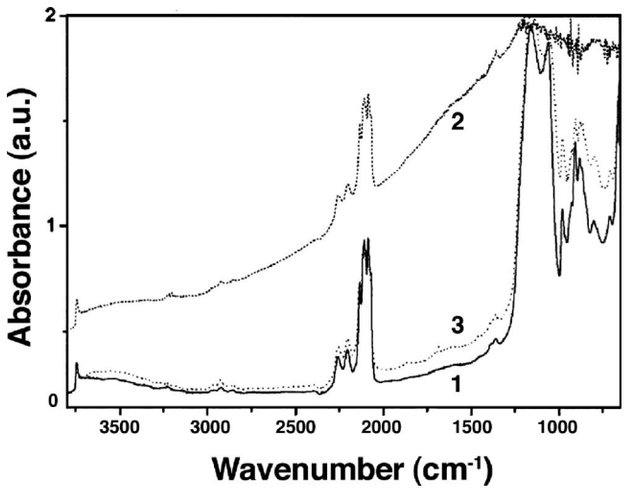

Figure 3. FTIR spectra of the mesoPS exposed to nitrogen dioxide. The solid line 1 is the fresh sample in the vacuum, the dashed line 2 is in the presence of 1 Torr of pure NO_2, and the dotted line 3 has been acquired after gas evacuation.

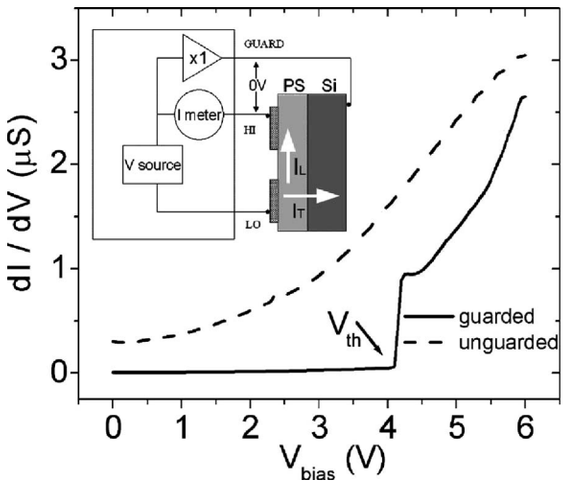

Figure 4. Differential conductance of a mesoPS sample (60% porosity). A gap characterized by a threshold voltage is clearly visible. When the guard is removed, the gap disappears. This is related to the structural anisotropy of mesoPS. The inset shows the measurement configuration.

comparative cases. NH_3, for instance, is well-known to a donorlike molecule, which is, to some extent, a behavior opposite to that of NO_2.

Other Techniques and Results

Since 1999, other groups contributed to the study of the NO_2 interaction with detailed papers on IR spectroscopy and the Drude effect due to the free carriers restored by NO_2 [12] and obtained different records of sensitivity (15 ppb in dry air).[25]

The main results of this period of fundamental investigations were the following:

1. mesoPS is, from an electrical point of view, a near insulator and becomes either a p- or an n-type semiconductor upon gas adsorption (NO_2 and NH_3).[22,24]
2. The interaction of these two probe gases is stronger than those typical of polar gases and liquids, and it can be well represented by an adsorption isothermal characteristic of a chemisorption mechanism.[24,26]
3. The effect of the free carrier's deactivation/reactivation is reversible at a low concentration of these two gases, and it is not due to a change in the coordination of the boron impurities at the mesostructure surface.[24]

Electrical Anisotropy and Coulomb Blockade

Since 2005, our work continued focusing the investigation on the electron transport phenomena of mesoPS in interaction with probe gases. Thanks to experimental setups, aspects of the complex phenomena were further understood and demonstrated.

The experimental setup shown in the inset of Fig. 4 allowed the demonstration of electrical anisotropy in p+ mesoPS morphology.[27] This anisotropy was first demonstrated by Forsh et al.[28] on a mesoPS obtained by (110) wafers [but for the (100) plane, this electrical characteristic was always given as an assumption and was never measured as two separated contributions] that are longitudinal (I_L) and transversal (I_T) to the direction perpendicular to (100) plane.

As depicted in Fig. 4, when a bias voltage is applied between the coplanar contacts, the measured current I is given by the sum of the longitudinal current I_L crossing the mesoPS from one pad to the other, i.e., parallel to the (100) plane and the leakage current I_T (unless the back-side contact is used as a guard electrode). In the latter, the same potential is kept on the back-side contact and on one planar contact so that no current flow occurs between them.

By measuring the samples in both the configurations, it is possible to separate the different conductivity contributions in a strongly anisotropic material such as p^+ mesoPS.

The room-temperature conductivity in the transverse direction is apparently percolated already, while the longitudinal direction is apparently strongly inhibited. This difference disappears by increasing the temperature along with a longitudinal conductivity rise in the orders of magnitude. The strong electrical anisotropy measured in this material gives further confirmation to the former results in 2001 of the increased sensitivity in the suspended PS membranes.

Furthermore, all the mesoPS samples under investigation, in guard electrode configuration, showed the presence of a sharp threshold voltage V_{th} in the current–voltage characteristics at room temperature. The typical gap in the conductance observed in a sample of 60% porosity is shown in Fig. 4. The threshold disappears as the guard contact is removed because the conductive pathways are restored again along the transversal direction. In this configuration, the bottlenecks constituted by the small nanoconstrictions are easily bypassed, and the transversal direction is over the percolation threshold. By investigating the shape and dependence of the threshold voltage with temperature variation from room temperature to 200 K, it was possible to understand the origin of the conductivity gap, identifying an increase in the threshold values with decreasing temperature and a power law behavior for the $V > V_{th}$ common to other metallic or semiconducting nanoparticle systems such as Co nanocrystal superlattices,[29] Au nanocrystal arrays,[30,31] GaAs quantum dots,[32] PbSe quantum dots,[33] C nanoparticle chains,[34] and polymer nanofibers.[35] Moreover, such a behavior was theoretically predicted by Middleton and Wingreen[36] for the collective transport in arrays of small metallic dots.

In conclusion, the conductivity gap could be due to the localization of positive charges in the nanoconstrictions, which can inhibit, by coulomb interaction, the whole current in the longitudinal direction, where the Si nanocrystals are poorly interconnected. Both the temperature and NO_2 are able to detrap holes, opening conductive pathways. Such interpretation is strictly connected to the surface effect scenario proposed by Lehmann. Moreover, the coulomb blockade effects in the electrical transport in PS were taken into account by Hamilton et al.[37] in 1998 but was never demonstrated before.

Finally, the most recent chapter of the story is the experimental observation of an intriguing time-dependent charge transport phe-

nomena, such as slow conductivity relaxation, nonergodicity, and simple aging at room temperature.[38] These phenomena have a deep impact on the transport in mesoPS and may affect the electrical response of the material to gases.

Conclusions

From the first electrical measurements in nitrogen dioxide atmosphere up to now, a basic research activity on mesoPS, its interaction with gases, and its transport properties has been carried out. Chemisorption mechanisms, free carrier reactivation and doping by gaseous species, and electrical anisotropy of $\langle 100 \rangle$ p^+ porous silicon have been evidenced and demonstrated, and moreover, coulomb blockade effects have been identified.

After 13 years of researching on these topics and over 3 years from his early departure, Lehmann's deep intuitions still hold true, and new areas of investigation are emerging thanks to the deeper comprehension gained following his first indications.

Istituto Nazionale di Ricerca Metrologica assisted in meeting the publication costs of this article.

References

1. T. Unagami, *J. Electrochem. Soc.*, **127**, 476 (1980).
2. M. I. J. Beale, J. D. Benjamin, M. J. Uren, N. G. Chew, and A. G. Cullis, *J. Cryst. Growth*, **73**, 622 (1985).
3. A. J. Read, R. J. Needs, K. J. Nash, L. T. Canham, P. D. J. Calcott, and A. Qteish, *Phys. Rev. Lett.*, **69**, 1232 (1992).
4. R. Tsu and D. Babic, *Appl. Phys. Lett.*, **64**, 1806 (1994).
5. V. Lehmann, F. Hofmann, F. Moeller, and U. Gruening, *Thin Solid Films*, **255**, 20 (1995).
6. L. T. Canham, in *Properties of Porous Silicon*, EMIS Data Review Series, L. T. Canham, Editor, p. 106, INSPEC, London, UK (1997).
7. M. Ben-Chorin, A. Kux, and J. Schechter, *Appl. Phys. Lett.*, **64**, 481 (1994).
8. G. Polisski, D. Kovalev, G. Dollinger, T. Sulima, and F. Koch, *Physica B*, **273**, 951 (1999).
9. E. H. Poindexter, P. J. Caplan, B. E. Deal, and R. R. Razouk, *J. Appl. Phys.*, **52**, 879 (1981).
10. H. J. von Bardeleben, D. Stievenard, A. Grosman, C. Ortega, and J. Siejka, *Phys. Rev. B*, **47**, 10899 (1993).
11. F. C. Rong, J. F. Harvey, E. H. Poindexter, and G. J. Gerardi, *Appl. Phys. Lett.*, **63**, 920 (1993).
12. V. Yu. Timoshenko, T. Dittrich, V. Lysenko, M. G. Lisachenko, and F. Koch, *Phys. Rev. B*, **64**, 085314 (2001).
13. J. Harper and M. J. Sailor, *Anal. Chem.*, **68**, 3713 (1996).
14. L. Boarino, C. Baratto, F. Geobaldo, G. Amato, E. Comini, A. M. Rossi, G. Faglia, G. Lérondel, and G. Sberveglieri, *Mater. Sci. Eng., B*, **69-70**, 210 (2000).
15. A. Halimaoui, in *Porous Silicon: Material Processing, Properties, and Applications*, J. C. Vial and J. Derrien, Editors, p. 33, Springer, New York (1994).
16. C. Baratto, G. Faglia, G. Sberveglieri, L. Boarino, A. M. Rossi, and G. Amato, *Thin Solid Films*, **391**, 261 (2001).
17. *EH40/2002 Occupational Exposure Limits – Supplement 2003*, Health and Safety Executive, Sudbury, Suffolk, UK (2003).
18. L. Francioso, A. Forleo, S. Capone, M. Epifani, A. M. Taurino, and P. Siciliano, *Sens. Actuators B*, **114**, 646 (2006).
19. Y. Ogata, H. Niki, T. Sakka, and M. Iwasaki, *J. Electrochem. Soc.*, **142**, 1595 (1995).
20. P. Rivolo, F. Geobaldo, M. Rocchia, G. Amato, A. M. Rossi, and E. Garrone, *Phys. Status Solidi A*, **197**, 217 (2003).
21. F. Geobaldo, P. Rivolo, M. Rocchia, A. M. Rossi, and E. Garrone, *Phys. Status Solidi A*, **197**, 458 (2003).
22. M. Chiesa, G. Amato, L. Boarino, E. Garrone, F. Geobaldo, and E. Giamello, *Angew. Chem., Int. Ed.*, **42**, 5031 (2003).
23. S. Borini and P. Ugliengo, *Phys. Status Solidi A*, **197**, 436 (2003).
24. E. Garrone, F. Geobaldo, P. Rivolo, G. Amato, L. Boarino, M. Chiesa, E. Giamello, R. Gobetto, P. Ugliengo, and A. Viale, *Adv. Mater.*, **17**, 528 (2005).
25. L. Pancheri, C. J. Oton, Z. Gaburro, G. Soncini, and L. Pavesi, *Sens. Actuators B*, **89**, 237 (2003).
26. F. Geobaldo, B. Onida, P. Rivolo, S. Borini, L. Boarino, A. M. Rossi, G. Amato, and E. Garrone, *Chem. Commun. (Cambridge)*, **2001**, 2196.
27. S. Borini, L. Boarino, and G. Amato, *Appl. Phys. Lett.*, **89**, 132111 (2006).
28. P. A. Forsh, M. N. Martyshov, V. Y. Timoshenko, and P. K. Kashkarov, *Semiconductors*, **40**, 471 (2006).
29. C. T. Black, C. B. Murray, R. L. Sandstrom, and S. Sun, *Science*, **290**, 1131 (2000).
30. H. Fan, K. Yang, D. M. Boye, T. Sigmon, K. J. Malloy, H. Xu, G. P. Lopez, and C. J. Brinker, *Science*, **304**, 567 (2004).
31. R. Parthasarathy, X.-M. Lin, K. Elteto, T. F. Rosenbaum, and H. M. Jaeger, *Phys. Rev. Lett.*, **92**, 076801 (2004).
32. C. I. Duruoz, R. M. Clarke, C. M. Marcus, and J. S. Harris, *Phys. Rev. Lett.*, **74**, 3237 (1995).
33. H. E. Romero and M. Drndic, *Phys. Rev. Lett.*, **95**, 156801 (2005).
34. A. Bezryadin, R. M. Westervelt, and M. Tinkham, *Appl. Phys. Lett.*, **74**, 2699 (1999).
35. A. N. Aleshin, H. J. Lee, S. H. Jhang, H. S. Kim, K. Akagi, and Y. W. Park, *Phys. Rev. B*, **72**, 153202 (2005).
36. A. A. Middleton and N. S. Wingreen, *Phys. Rev. Lett.*, **71**, 3198 (1993).
37. B. Hamilton, J. Jacobs, D. A. Hill, R. F. Pettifer, D. Teehan, and L. T. Canham, *Nature (London)*, **393**, 443 (1998).
38. S. Borini, L. Boarino, and G. Amato, *Phys. Rev. B*, **75**, 165205 (2007).